SPECIAL ISSUE REVIEW ARTICLE

WILEY NMR IN BIOMEDICINE

Advanced single voxel ^{1}H magnetic resonance spectroscopy techniques in humans: Experts' consensus recommendations

Gülin Öz[1] | Dinesh K. Deelchand[1] | Jannie P. Wijnen[2] | Vladimír Mlynárik[3] | Lijing Xin[4] | Ralf Mekle[5] | Ralph Noeske[6] | Tom W.J. Scheenen[7,8] | Ivan Tkáč[1] | the Experts' Working Group on Advanced Single Voxel ^{1}H MRS

[1] Center for Magnetic Resonance Research, Department of Radiology, University of Minnesota, Minneapolis, USA

[2] High Field MR Research group, Department of Radiology, University Medical Centre Utrecht, Utrecht, the Netherlands

[3] High Field MR Centre, Department of Biomedical Imaging and Image-Guided Therapy, Medical University of Vienna, Vienna, Austria

[4] Animal Imaging and Technology Core (AIT), Center for Biomedical Imaging (CIBM), École Polytechnique Fédérale de Lausanne, Lausanne, Switzerland

[5] Center for Stroke Research Berlin (CSB), Charité Universitätsmedizin Berlin, Berlin, Germany

[6] GE Healthcare, Berlin, Germany

[7] Department of Radiology and Nuclear Medicine, Radboud University Medical Center, Nijmegen, the Netherlands

[8] Erwin L. Hahn Institute for Magnetic Resonance Imaging, UNESCO World Cultural, Heritage Zollverein, Essen, Germany

Correspondence
Gülin Öz, Center for Magnetic Resonance Research, University of Minnesota, 2021 Sixth Street Southeast, Minneapolis, MN 55455.
Email: gulin@cmrr.umn.edu

Conventional proton MRS has been successfully utilized to noninvasively assess tissue biochemistry in conditions that result in large changes in metabolite levels. For more challenging applications, namely, in conditions which result in subtle metabolite changes, the limitations of vendor-provided MRS protocols are increasingly recognized, especially when used at high fields ($\geq$3 T) where chemical shift displacement errors, B_0 and B_1 inhomogeneities and limitations in the transmit B_1 field become prominent. To overcome the limitations of conventional MRS protocols at 3 and 7 T, the use of advanced MRS methodology, including pulse sequences and adjustment procedures, is recommended. Specifically, the semiadiabatic LASER sequence is recommended when T_E values of 25-30 ms are acceptable, and the semiadiabatic SPECIAL sequence is suggested as an alternative when shorter T_E values are critical. The magnetic field B_0 homogeneity should be optimized and RF pulses should be calibrated for each voxel. Unsuppressed water signal should be acquired for eddy current correction and preferably also for metabolite quantification. Metabolite and water data should be saved in single shots to facilitate phase and frequency alignment and to exclude motion-corrupted shots. Final averaged spectra should be evaluated for SNR, linewidth, water suppression efficiency and the presence of unwanted coherences. Spectra that do not fit predefined quality criteria should be excluded from further analysis. Commercially available tools to acquire all data in consistent anatomical locations are recommended for voxel prescriptions, in particular in longitudinal studies. To enable the larger MRS community to take advantage of these advanced methods, a list of resources for these advanced protocols on the major clinical platforms is provided. Finally, a set of recommendations are provided for vendors to enable development of advanced MRS on standard platforms, including implementation of advanced localization sequences, tools for quality assurance on the scanner, and tools for prospective volume tracking and dynamic linear shim corrections.

KEYWORDS

body, brain, chemical shift displacement, metabolites, reproducibility, semiadiabatic LASER, shimming, SPECIAL

1 | INTRODUCTION

Proton magnetic resonance spectroscopy (^{1}H MRS) provides a wealth of biochemical and metabolic information complementary to conventional structural MRI. An international consensus effort[1] documented the impact of ^{1}H MRS in the clinical evaluation of brain tumors, childhood neurological diseases, demyelinating disorders and brain infections, primarily based on work at 1.5 T. Metabolite abnormalities in these "clinic-ready" applications are detectable in individual patients with conventional, vendor-provided MRS packages. In addition, consensus was reached that conventional MRS protocols are severely limited for more challenging applications with subtler metabolite changes, especially when used at high (3 T) and ultrahigh fields (7 T and higher). The MRS community then followed up with a second technical consensus statement, which declared the localization error of the widely used PRESS sequence at 3 T as unacceptable and recommended the use of the semiadiabatic localization by adiabatic selective refocusing (sLASER) sequence as a solution.[2]

To detail the benefits of such advanced MRS methodology at high and ultrahigh fields and to facilitate wider access to these methods, the current paper was prepared by a group of experts who developed, implemented and optimized such advanced MRS protocols on clinical platforms. These authors provided recommendations on how to use the technology, which were then reviewed and endorsed by a larger group of investigators who have expertise in advanced single voxel spectroscopy (SVS) techniques (the members of the larger group are listed in Table S1).

First, we summarize the demands brought by high fields that necessitate the use of advanced MRS protocols for human subject applications and demonstrate the improvements that advanced MRS protocols provide over conventional protocols. Note that an advanced SVS protocol not only includes a localization sequence that provides accurate localization within the B_1 constraints of high fields, but also provides efficient water suppression, incorporates voxel-based B_0 and B_1 adjustments, as well as measures taken to mitigate motion artifacts. For the localization aspect, we focus on two pulse sequences that have been widely used in advanced MRS protocols at high and ultrahigh fields: (a) sLASER, which was recommended in the technical consensus statement,[2] and (b) the spin echo full intensity acquired localized (SPECIAL) spectroscopy sequence, which has been used by a number of groups and provides advantages over sLASER in certain applications. For readers interested in using advanced SVS sequences, we provide a list of available sources to access these sequences (Table S2). We provide recommendations to assist users to select the field strength and pulse sequence for different applications and guidelines for quality assurance (QA, prospective measures taken to acquire high quality data) and quality control (QC, retrospective measures taken to identify and eliminate poor quality data). We further provide recommendations to MR scanner vendors to enable users to acquire high quality MRS data at high and ultrahigh fields. Note that edited MRS has been intentionally left out of this paper since it is covered in a separate contribution in this special issue.[3]

# 2 | THE NEED FOR ADVANCED SVS PROTOCOLS AT HIGH FIELD

High and ultrahigh fields introduce technical challenges that can be overcome using advanced protocols for optimal SVS data quality, as described below. The first challenge, chemical shift displacement error (CSDE), is addressed with sequence and radiofrequency (RF) pulse selection, while the challenges associated with B_1 and B_0 inhomogeneity are addressed by voxel-based calibrations, which are recommended for all localization sequences at high field.

2.1 | Chemical shift displacement error

The chemical shift difference between different resonances causes a CSDE when a magnetic field gradient is used in combination with a frequency-selective RF pulse to selectively excite, refocus or invert a slice. The combination of the bandwidth of the RF pulse, the chemical shift of the metabolite of interest, the transmitter frequency and the strength of the magnetic field gradient define the exact position of slice selection for each resonance (Figure 1). The CSDE between two resonances is expressed as a percentage of the voxel size, and is given by the ratio of the chemical shift difference (in Hz) between the two resonances of interest and the bandwidth of the frequency-selective pulse. The CSDE is present in each direction in which slice selection is used for excitation, refocusing or inversion. The CSDE often leads to unacceptably large differences in the localization of different resonances (>30% for the 3 ppm range of the spectrum in one dimension) with conventional MRS sequences that utilize RF refocusing pulses with small bandwidths, even at 3 T (Figure 1). Moreover, molecules with spin systems that have coupled resonances far apart in the ppm scale, such as lactate with an internal chemical shift difference of 2.8 ppm, may experience intravoxel shape distortions and signal loss because of small bandwidth slice-selective refocusing.[4] Therefore, sequences that utilize RF pulses with sufficiently broad bandwidths to minimize CSDE are essential at 3 T and higher fields.[2]

2.2 | B_1 inhomogeneity

The RF pulses for excitation and refocusing of ^{1}H spins use frequencies that in tissue have wavelengths of the order of the size of the human head at high magnetic fields, causing interference effects. Together with attenuation of these RF pulses by conductive tissue, the resulting magnetic
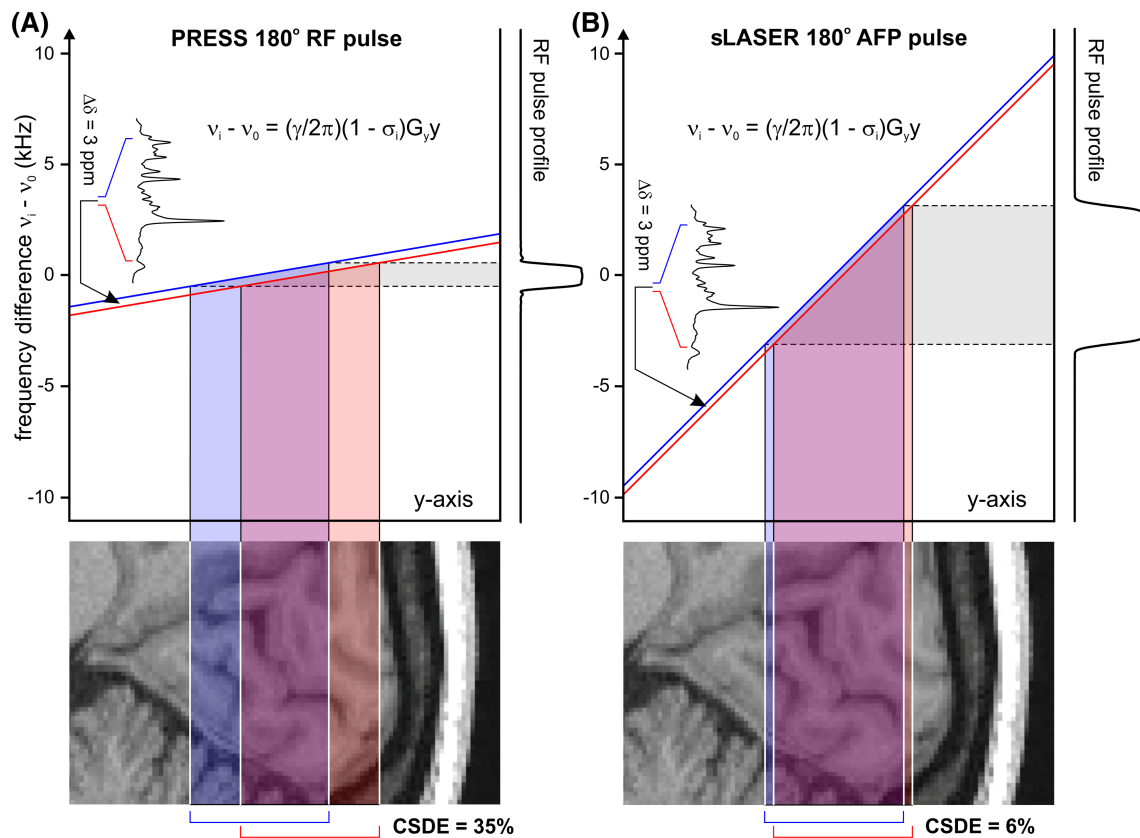
FIGURE 1 Comparison of the chemical shift displacement error (CSDE) between point-resolved spectroscopy (PRESS) and semiadiabatic LASER (sLASER) pulse sequences at 3 T. Only the displacement along the slice experiencing 180° refocusing pulse is shown (the y-axis was chosen for this CSDE illustration). Plots in (A) and (B) demonstrate the spatial dependences of resonance frequencies for two resonances separated by 3 ppm (370 Hz at 3 T) for PRESS and sLASER, respectively. The vertical axis represents the field strength; the scale is expressed in frequency units (kHz) and shows the difference from the resonance frequency $\nu_0 = (\gamma/2\pi) B_0$. A typical narrow bandwidth of PRESS 180° pulse (1.06 kHz) translates into 35% CSDE (per 3 ppm) in one direction. Substantially increased bandwidth of adiabatic full passage (AFP) 180° pulse in sLASER (6.3 kHz) reduces the CSDE to 6% (per 3 ppm). The displacement of slices is shown on sagittal MRI of human brain zoomed at occipital lobe

field B_1^+ of the pulses is inhomogeneous across the brain and body at high fields, despite the use of volume RF excitation coils.[5,6] Depending on the size and location of a spectroscopic volume of interest (VOI), this inhomogeneity can cause intravoxel variation of flip angles (in large volume selections) or a bias in the intended flip angle for a particular voxel location. While intravoxel RF inhomogeneity can usually be neglected for small voxel volumes (~ a few cm³) in SVS, inaccurate flip angles for the selected VOI are common in conventional MRS protocols that use flip angles obtained from slice-based calibrations.[7] Inaccurate flip angles in turn lead to changes in the VOI shape, incomplete refocusing, loss of SNR and unwanted coherences due to excitation outside the intended VOI (Figure 2). The B_1^+ inhomogeneity at high fields is primarily a concern when using nonadiabatic RF pulses; however, it can degrade SNR and induce unwanted coherences even when adiabatic pulses are used because pulse sequences typically operate near the limit of adiabaticity at high and ultrahigh fields. Therefore, voxel-based flip angle calibration is necessary at 3 T and above for accurate localization, optimum SNR and efficient artifact suppression.

2.3 | B_0 inhomogeneity

Inhomogeneities in the static magnetic field B_0 also increase with increasing magnetic field[8] and, if not compensated properly, result in broad linewidths and compromised SNR. Broader lines in turn increase spectral overlap preventing reliable separation of metabolites such as glutamate and glutamine in the brain, which are then reported as a sum (ie, glutamate + glutamine [Glx]). Therefore, adjustment of both first- and second-order shims in the selected VOI is particularly important at high and ultrahigh fields. While vendor-provided advanced 3D shimming routines continually improve, they may not provide the narrowest linewidths achievable in all potential regions of interest (Figure 3).[7]

(A)

(B)
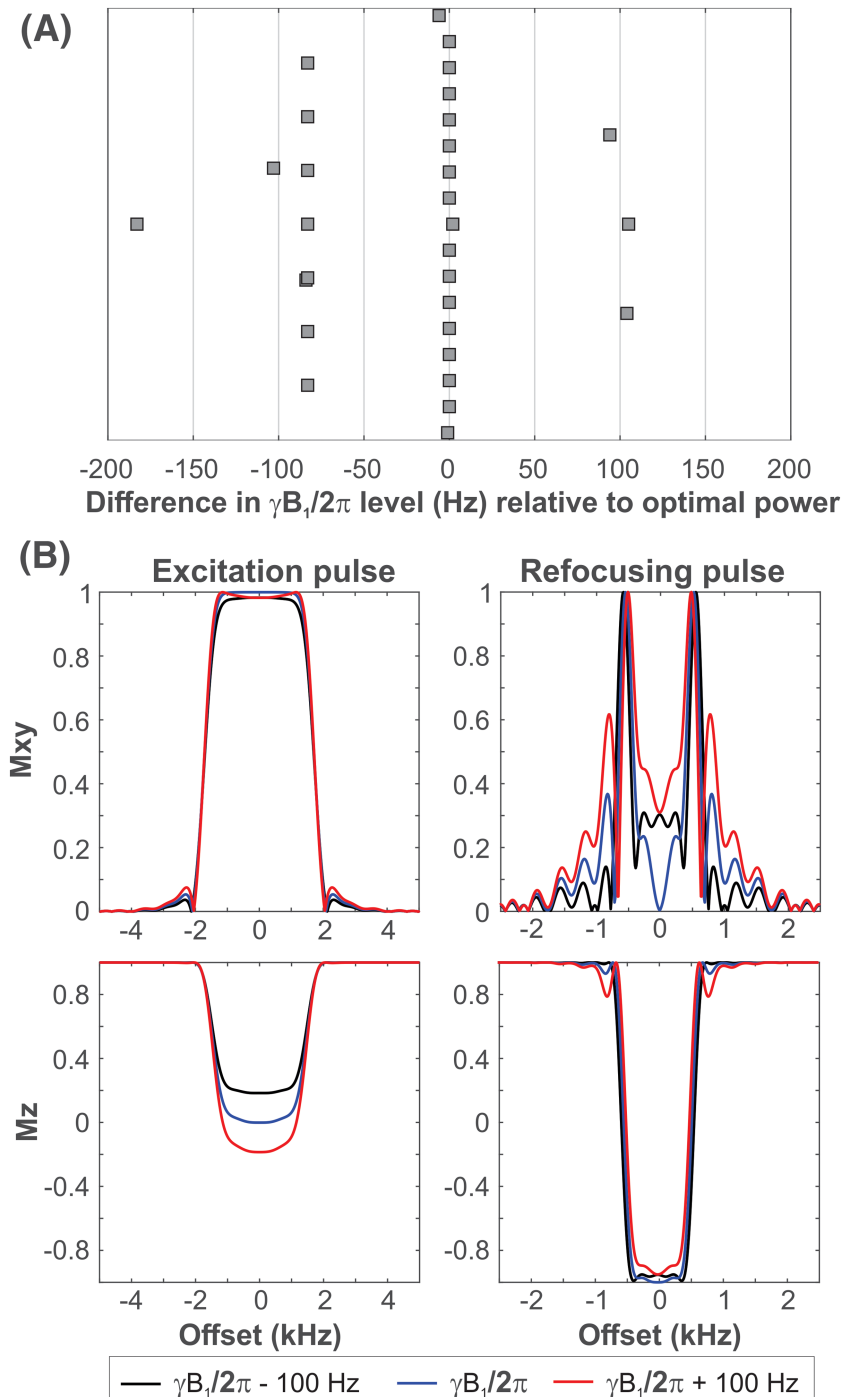
FIGURE 2 Effect of inaccurate B_1 calibration. (A) The difference in B_1 level measured using system slice-based prescan calibration and voxel-based calibration. Data were acquired from 30 subjects at 3 T. The B_1 was miscalibrated in more than 40% of the subjects with the slice-based prescan and the difference from the voxel-based calibration ranged from -183 to +105 Hz. (B) The effect of underestimated and overestimated B_1 relative to optimal B_1 on the radiofrequency (RF) profiles are illustrated for an excitation pulse (2.6 ms Hamming sinc pulse) and a refocusing pulse (5.4 ms Mao pulse) typically used in point-resolved spectroscopy (PRESS). A difference of 100 Hz from optimal $\gamma B_1/2\pi$ (846 Hz for the excitation pulse and 1010 Hz for refocusing pulse), which was typical for the data in shown in (A), was chosen for this simulation

3 | TECHNICAL OVERVIEW OF TWO WIDELY USED ADVANCED SVS SEQUENCES

Here, we focus on the sLASER and SPECIAL protocols as these are the most widely used and validated advanced sequences at high and ultrahigh fields, and their commonly used protocols (including prescan calibrations, optimized localization sequence and postacquisition processing) address the challenges brought by high fields. Their features are compared with the conventional MRS pulse sequences, namely, stimulated echo acquisition mode (STEAM)[9] and point-resolved spectroscopy (PRESS),[10,11] which are available in standard MRS packages on all clinical MR platforms (Table 1). Note that optimized versions of STEAM that provide ultrashort T_E (<10 ms) and better localization performance[13] are available as research packages (Table S2). Similarly, the CSDE of PRESS can be substantially improved in the OVERPRESS sequence with very selective saturation pulses, which was recommended in the technical consensus statement as an alternative at 3 T if sLASER is not available.[2]
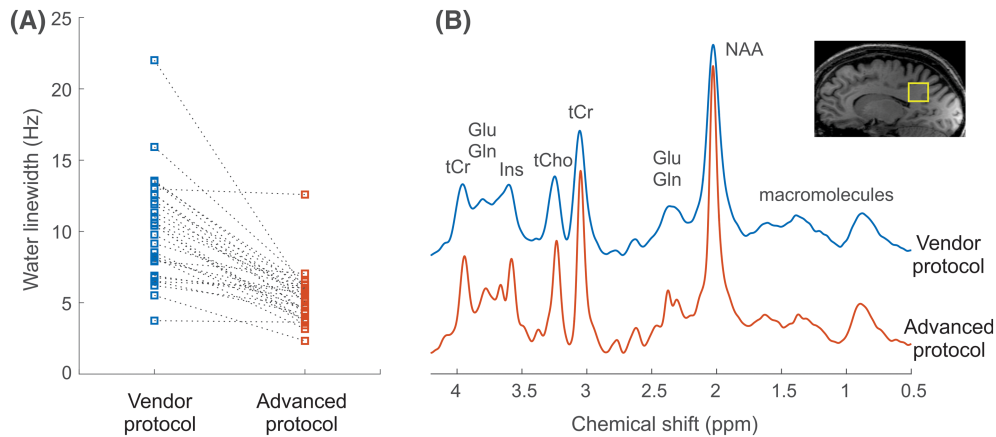
FIGURE 3 B_0 shim performance using a vendor-provided shimming routine (3D gradient echo) and a work-in-progress advanced shimming tool (FASTMAP) on a Siemens Verio 3 T scanner. (A) Individual water linewidths measured from 30 subjects using both B_0 shim techniques are illustrated. Narrower linewidths were achieved using FASTMAP (5 ± 2 Hz) compared with system shim (10 ± 4 Hz). (B) Point-resolved spectroscopy (PRESS) spectra (volume of interest [VOI] = 20 x 20 x 20 mm^3, T_R/T_E = 5000/30 ms, number of transients (NT) = 64, T_{acq} = 819 ms and number of points = 2048) acquired from posterior cingulate cortex in the same subject using the two shimming techniques at 3 T. Data processing consisted of zero-filling up to 8-k data points, Gaussian multiplication of the free induction decay (FID) (σ = 0.12/second), Fourier transformation and phase correction. The inset shows the location of the MRS voxel on the T_1-weighted image. This example illustrates the effect of the shimming performance on spectral quality. In this case, the advanced shimming tool outperformed the system shim due to the coarse resolution of the field map obtained with the system shim

3.1 | The sLASER sequence

An important tool to overcome the challenges associated with CSDE is the use of adiabatic RF pulses. The initial idea of accurate volume localization in SVS with seven adiabatic pulses[14] evolved into the full LASER pulse sequence,[15] of which the first three pulses were later replaced by one conventional nonadiabatic slice-selective excitation pulse.[16] The sLASER sequence is a single-shot, full-intensity spectroscopic method that uses a slice-selective excitation pulse followed by two orthogonal pairs of slice-selective adiabatic full passage (AFP) pulses.[17] Typically, the shortest T_E ranges from 25 to 30 ms at 3 and 7 T.[16-19] To improve localization, especially in the slice excitation direction, sLASER is usually combined with outer volume suppression (OVS) modules prior to the localization sequence.[16-18] Finally, the variable pulse power and optimized relaxation delays (VAPOR) scheme[20] is typically interleaved with the OVS modules (Figure 4A).[17,18] sLASER provides several advantages over STEAM[9] and PRESS[10,11] (Table 1): (a) it retains full intensity as opposed to STEAM, which only retains half of the available signal; (b) the CSDE of the refocusing pulses is much smaller (<4% per ppm) than in PRESS due to the high bandwidth of the AFP pulses (typically >5 kHz); (c) it provides clean and sharp slice-selection profiles for accurate localization; and (d) the pairs of AFP pulses act as a Carr-Purcell[21] pulse train to suppress J-modulation in J-coupled metabolites and also to lengthen the apparent transverse relaxation times of water and metabolites.[22,23] In comparison with the full LASER sequence, sLASER allows shorter T_E, which increases the SNR and reduces the sensitivity to metabolite T_2 relaxation times. In addition, the slice-selective excitation used in sLASER reduces the possibility of spurious echoes relative to the whole volume excitation used in LASER. The limitations of sLASER are (a) the necessity to use refocusing pulses in pairs to remove the quadratic phase of the adiabatic pulse across a slice profile, and (b) the associated RF power deposition limiting the choice for short repetition times, especially at high field. The use of gradient-modulated RF pulses, such as FOCI or GOIA pulses,[24,25] with lower $B_1^+(max)$ requirements than hyperbolic secant adiabatic pulses for a given bandwidth, recently enabled short T_E sLASER implementations on 3 T systems with a limit on maximum available $B_1^+(max)$.[26]

3.2 | The SPECIAL and semiadiabatic SPECIAL sequences

The SPECIAL spectroscopy sequence[12] was designed to acquire full intensity signal in a specified VOI at an ultrashort T_E of ~ 5-9 ms on a clinical platform. This hybrid pulse sequence[27] (Figure 4B) combines localization in one direction by the 1D image-selected in vivo spectroscopy (ISIS) technique[12] with a slice-selective spin-echo sequence for localization in the other two directions, allowing for an ultrashort T_E. ISIS localization is typically achieved with an adiabatic inversion pulse, and any unwanted transverse magnetization created by the inversion pulse is efficiently removed by a spoiling gradient in the time delay between the ISIS and spin echo modules. During this delay, magnetization is conserved along the static magnetic field. Thus, this delay does not contribute to the overall echo time of the sequence. Similar to the sLASER

TABLE 1 Comparison of features of product versus advanced MRS pulse sequences

Sequence characteristics	Vendor product sequences[a]		Advanced MRS sequences[a]			
	STEAM[b]	PRESS[c]	sLASER[d]		SPECIAL[e]	sSPECIAL[f]
Fraction of available signal	50%	100%	100%		100%	100%
Localization performance[g]	++	+	++++		+++	++++
Profiles of RF pulses[g]	++	+	++++		+++	++++
Sensitivity to B_1 inhomogeneity[h]	- -	- - - -	-		- -	-
Single shot method	yes	yes	yes		no	no
Sensitivity to motion[h]	-	-	-		- - -	- - -
Performance at 7 T with standard hardware[g,i]	+	poor	+++		poor	++
3 T (for brain applications):						
Minimum TE (body transmit coil)	9-20 ms	30 ms	30 ms[j]	23 ms	8.5 ms	16 ms
Required B_1^+(max)	14-20 µT	24 µT	15 µT[j]	25 µT	24 µT	24 µT
CSDE/ppm – slice #1[k]	4%-5%	4%	5%[j]	3%	4%	2%
CSDE/ppm – slice #2[k]	4%-5%	12%	1%[j]	1%	3%	3%
CSDE/ppm – slice #3	4%-5%	12%	1%[j]	1%	12%	2%
7 T (for brain applications):						
Minimum TE (head transmit volume coil)	14-20 ms	30 ms	26 ms		8.5 ms	16 ms
Required B_1^+(max)	14-20 µT	24 µT	26 µT[l]		24 µT	24 µT
CSDE/ppm – slice #1[k]	9%-12%	9%	7%		11%	6%
CSDE/ppm – slice #2[k]	9%-12%	28%	3%		7%	7%
CSDE/ppm – slice #3	9%-12%	28%	3%		28%	6%

[a]Features and values provided for stimulated echo acquisition mode (STEAM) and point-resolved spectroscopy (PRESS) are typical for vendor MRS packages. In-house implementations of these sequences typically have improved features, such as shorter TE for STEAM. Features and values provided for advanced MRS sequences are for current implementations available to the MRS community via work-in-progress packages or customer-to-customer sequence sharing. Further improvements in utilized radiofrequency (RF) pulses are possible and encouraged in future implementations.

[b]Using Hamming sinc pulses.

[c]Using Hamming sinc pulses for excitation and Mao pulses for refocusing.

[d]Using asymmetric sinc pulse for excitation and gradient offset independent adiabatic (GOIA)-WURST pulses for refocusing.

[e]Using asymmetric sinc pulse for excitation, hyperbolic secant adiabatic pulse (HS1) for inversion and Mao pulse for refocusing.

[f]Semiadiabatic spin echo full intensity acquired localized spectroscopy (SPECIAL), using asymmetric sinc pulse for excitation and hyperbolic secant adiabatic pulses (HS4) for inversion and refocusing.

[g]Larger number of + signs indicate positive attributes, eg, better localization performance. The evaluation of the localization performance considers the sequences as currently implemented, including outer volume suppression (OVS) modules.

[h]Larger number of - signs indicate negative attributes, eg, higher sensitivity to B_1 inhomogeneities and motion.

[i]Standard 7 T hardware refers to widely used commercial coils, such as transmit volume coils for brain applications. Performance with respect to shortest attainable TE and chemical shift displacement error (CSDE) improves with use of surface or half-volume coils that can deliver higher B_1^+(max). The poor performance evaluation is primarily based on high CSDE and poor excitation profiles of radiofrequency (RF) pulses used in the pulse sequences.

[j]While most clinical 3 T scanners provide ~ 25 µT B_1^+(max) using standard body coil transmit, some 3 T platforms impose a software constraint on the maximum available B_1^+. Therefore, a harmonized semiadiabatic LASER (sLASER) sequence was recently implemented within a B_1^+(max) of 15 µT at 3 T.[26] The TE and CSDE values of that sequence are provided in this column.

[k]Slice #1 is excitation direction for STEAM, PRESS and sLASER, while slice #2 is excitation direction for SPECIAL and semiadiabatic SPECIAL (sSPECIAL).

[l]This B_1^+ level is achieved with a single channel transmit volume RF coil in the center of the head, similar B_1^+ values are achieved in the periphery with the use of dielectric padding.

protocol, OVS bands are interleaved with the VAPOR water suppression scheme[20] before the ISIS module to ensure the acquisition of artifact-free spectra.

The advantages of SPECIAL in comparison with conventional sequences for localized MRS (Table 1) are: (a) the method preserves the full magnetization available in the selected volume, (b) the shortest echo time achievable with this pulse sequence is comparable with that of STEAM, and (c) the adiabatic inversion pulse used for localization in one direction reduces the B_1 dependence of the obtained signal and provides
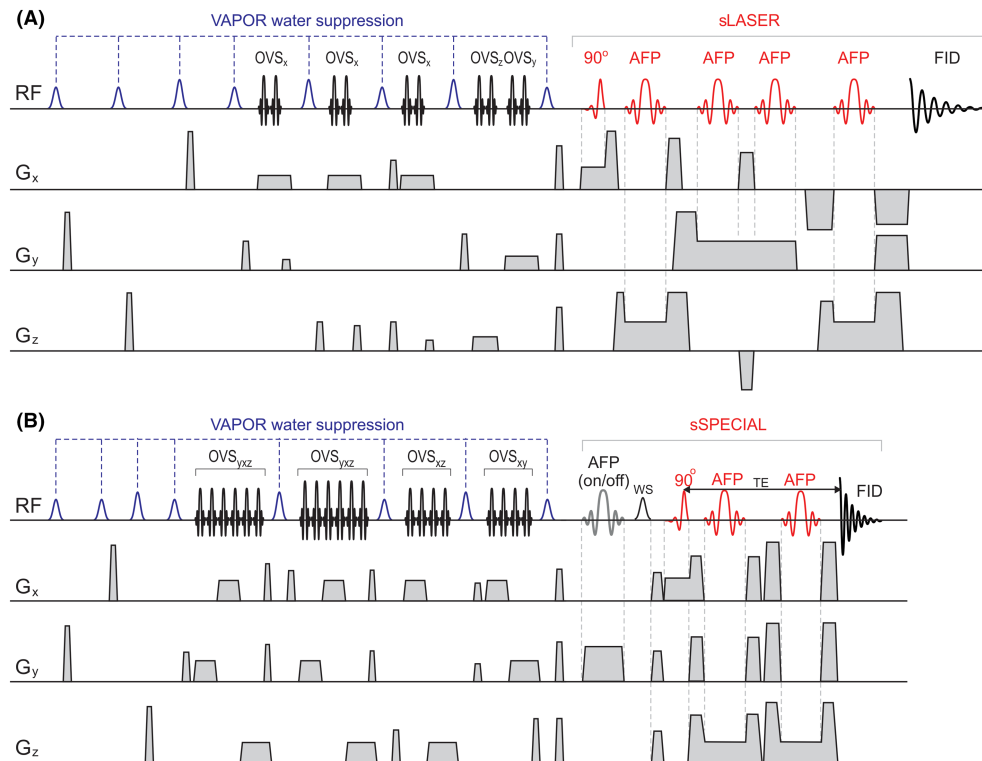
FIGURE 4 (A) Schematic diagram of the semiadiabatic LASER (sLASER) pulse sequence. In this variant of the sequence, the slice-selective 180° adiabatic full passage (AFP) pulses for selecting two dimensions are interleaved to minimize T_E. Three pairs of outer volume suppression (OVS) pulses are applied in the X-dimension selected by the slice-selective excitation pulse while single pairs of OVS pulses are applied in the Y- and Z-dimensions. The OVS modules are interleaved with VAPOR water suppression. Reproduced from[17] with permission from John Wiley and Sons. (B) Schematic diagram of the semiadiabatic SPECIAL (sSPECIAL) pulse sequence. The adiabatic inversion pulse is applied in alternate scans, together with alternating phase of the receiver. The slice-selective 90° pulse is asymmetric. Slice-selective 180°AFP pulses are used to select the third dimension. Water suppression (VAPOR) is interleaved with OVS, and an additional water suppression pulse (WS) is applied between the inversion pulse and the spin echo part of the sequence

homogeneous inversion, which is especially important when a surface coil is used as a transmitter. A drawback of SPECIAL is the necessity to use at least two scans, because full localization is achieved by subtracting two subsequent FIDs. This makes the method sensitive to any motion of the subject or any change between acquisitions of the two FIDs (eg, scanner drift). Thus, we recommend localized RF calibration, OVS and careful fixation of the subject when using SPECIAL.

The technique was implemented on a clinical platform at 3 and 7 T[28]; pulse types and durations were optimized for different RF coils and to address limitations in RF peak power and specific absorption rate (SAR) regulations.[29] Finally, the CSDE for the original version of the sequence was unacceptably high along the refocusing dimension at 3 T and, in particular, at 7 T relative to the recently recommended 4% per ppm level.[2] Therefore, a semiadiabatic version of SPECIAL (sSPECIAL) was developed to reduce the CSDE in the dimension selected by a conventional 180° pulse to acceptable levels, albeit at a somewhat longer T_E (Table 1).[30-32] If T_Es below 10 ms are of high interest, and a transmit RF coil which provides high B_1^+ amplitude (eg, a surface coil) is available, then the original sequence may still be used at 3 T. However, for all other scenarios and for use at 7 T, the sSPECIAL[31] sequence is preferred over the original SPECIAL sequence for human applications.

4 | RECOMMENDATIONS FOR ACQUISITION, ANALYSIS AND REPORTING OF ADVANCED SVS

The recommendations provided below pertain to both brain and body applications. Obtaining high quality MR spectra from the body presents additional challenges relative to the brain, which stem from: (a) the presence of more fat in the body compared with brain tissue and multiple fat-water transitions close to or even inside the VOI; (b) inhomogeneous B_1^+ fields in the body; (c) substantial organ movement due to respiratory and bowel motion; and (d) orientation-dependent resonance splitting due to dipolar coupling in muscle. Where necessary, alternative recommendations to address these additional challenges are noted in sections 4.1-4.3. The primary recommendations for data acquisition with advanced SVS protocols and for analysis of these data are summarized in Tables 2 and 3.

TABLE 2 Summary recommendations for data acquisition with advanced MRS protocols

Aspect	Recommendation
Field strength	• Sensitivity of 3 T sufficient for the most reliably quantified metabolites, eg, tNAA, tCr, tCho and *myo*-inositol in the brain in volume of interest (VOI) ≥ 4 mL • 7 T preferred for weakly represented metabolites and small VOI, but the B_0 and B_1 spatial inhomogeneity, limitations on available B_1^+(max), chemical shift displacement error (CSDE) and specific absorption rate (SAR) should be addressed • In both cases, establish test-retest reproducibility (preferred) or minimally quantitative error estimates in spectra obtained from the targeted VOI prior to study commencement
Radiofrequency (RF) coil	• 3 T: body transmit RF coils and multichannel receive arrays • 7 T: use commercial single channel transmit and multichannel receive arrays, with dielectric padding for peripheral VOI; for superficial VOI and if whole brain structural images are not needed, half-volume or surface coil transmitter can be used; when available, multichannel transmit coils should be used with B_1^+ shimming
Localization sequence (for standard hardware, eg, for body coil transmit at 3 T)	• Semiadiabatic LASER (sLASER) if T_E = 25-30 ms acceptable • Semiadiabatic SPECIAL (sSPECIAL) if T_E < 25 ms is critical • Ultrashort T_E stimulated echo acquisition mode (STEAM), if cohort is prone to motion and if the signal-to-noise ratio (SNR) of individual transients >3
VOI selection	• Use commercially available tools, eg, AutoAlign, SmartExam, to acquire images in the same reference frame in all subjects/sessions to improve consistency of manual VOI prescriptions and to save and retrieve VOI information in longitudinal scans of the same subject
B_0 adjustment	• Adjust first- and second-order shims for the targeted VOI using fully automated B_0 field mapping techniques, based on 3D B_0 mapping or mapping along projections • For body applications, shim on the water signal (not lipid) and correct carrier frequency after shimming
B_1 adjustment	• Calibrate flip angle for the targeted VOI
Water reference	• Acquire unsuppressed water signal from the same VOI, with carrier frequency on water, with the same gradients as the metabolite acquisition (for eddy current correction) and without outer volume suppression (OVS) (for quantification, to prevent MT effects), before metabolite acquisition
Metabolite acquisition	• Evaluate water linewidth before starting metabolite acquisition, repeat B_0 adjustment if linewidth is poor (>13 Hz at 3 T and >19 Hz at 7 T for brain) • Save single shots • Evaluate water suppression efficiency, spectral linewidth and SNR during acquisition, repeat acquisition if substantial motion is detected • Consider prospectively gated acquisitions for spine and body applications • Use prospective volume tracking methods whenever available

TABLE 3 Summary recommendations for analysis of data acquired with advanced MRS protocols

Aspect	Recommendation
Preprocessing steps	• Align phase and frequency of single shot spectra • Exclude transients corrupted by motion, average the remaining transients • Eliminate residual eddy current effects using the unsuppressed water signal
Quality control	• Evaluate spectra for linewidth; for brain applications exclude those with associated water linewidth >13 Hz at 3 T and >19 Hz at 7 T; for exclusion criteria in different organs, see[33] • Evaluate water suppression efficiency; exclude spectra where residual water distorts the spectral baseline or remove residual water peak in preprocessing • Evaluate signal-to-noise ratio (SNR); exclude those spectra with a SNR lower by a predefined factor compared with the average SNR of spectra in a study • Evaluate spectra for presence of unwanted coherences and distorted lipid signals, exclude spectra with substantial unwanted coherences or lipid signal contamination in the range of spectral fitting (typically ~ 4.2-0.5 ppm)
Quantification	• Fit-averaged, nonapodized spectra using automated packages for linear combination model fitting • Use a basis set generated with the data acquisition parameters (radiofrequency [RF] pulse shapes and timing), the basis set should also include an experimentally acquired macromolecule basis spectrum • Use quantitative error estimates, eg, Cramér-Rao lower bound (CRLB), when deciding on which metabolites are quantified reliably; avoid excluding individual concentrations based on relative CRLB; instead use CRLB thresholds (either mean CRLB or CRLB achieved in majority of spectra) to select metabolites that are most reliably quantified or consider using absolute CRLBs

4.1 | Choice of field strength and RF coil

When the study or clinical question primarily focuses on the most reliably quantifiable metabolites, such as tNAA, tCr, tCho, *myo*-inositol and glutamate in the brain, the sensitivity and resolution of 3 T will probably be sufficient for advanced SVS since the test-retest reproducibility at 3 T is currently equivalent to that at 7 T (between-session CVs of $\leq$5%-6%)[34-36] for VOI $\geq$ ~ 4 mL with advanced protocols. The advantages of 3 T scanners are that their hardware platforms are longer established and more stable and that they have fewer limitations on B_1^+(max), B_0 and B_1 spatial homogeneity, CSDE and SAR than 7 T scanners. On the other hand, if the focus is on weakly represented metabolites with *J*-coupled spin systems or severely overlapping resonances and small VOI (< ~ 4 mL), 7 T should be used when available, and so long as the B_0 and B_1 spatial inhomogeneities and limitations on available B_1^+(max), CSDE and SAR are successfully addressed (see the guidelines below for addressing these challenges). For example, while glutamate and glutamine can be distinguished reliably with advanced protocols in many brain regions at 3 T, Glx may need to be reported in VOI at challenging locations in the brain with low SNR and/or broad linewidths, while acquisitions at 7 T may allow their reliable separation. Consistently, the test-retest reproducibility advantages at 7 relative to 3 T are observed primarily for *J*-coupled metabolites such as glutamate, glutamine and glutathione.[34]

Whenever feasible, we recommend establishing test-retest reproducibility in the targeted VOI, with the chosen protocol, in a few healthy subjects prior to commencing a study. At a minimum, Cramér-Rao lower bounds (CRLB, see below) should be examined in sample spectra from the VOI chosen for the research question or the clinical examination. The absolute CRLB (as opposed to relative) are especially important when SVS is utilized in a clinical situation where, in most cases, decisions are based upon a single measurement.[37]

For 3 T, commercially available body transmit RF coils and multichannel receive arrays are recommended. At 7 T, widely available single channel transmit and multichannel receive arrays are recommended in conjunction with dielectric padding for the brain.[38,39] If the region of interest is superficial and whole brain imaging is not needed, the use of surface coils for transmission[12,28,40] is recommended to maximize B_1^+. If available, multichannel transmit coils and local B_1^+ shimming[41-43] should be used for optimal RF delivery. For applications in the torso at 7 T, the latter is essential.

4.2 | Choice of pulse sequence: How to minimize CSDE

An overview of widely used advanced SVS sequences and how they compare with conventional product sequences is provided in Table 1. The MRS Consensus Group recommended the use of sLASER instead of PRESS for substantially improved localization performance at 3 T and higher fields.[2] We support this recommendation because sLASER provides spectra that allow reliable quantification of a large number of metabolites at short T_E with minimal CSDE. In addition, as a single-shot method, sLASER allows correction of motion-related variations in frequency and phase. For applications where T_2 relaxation during a T_E of 25-30 ms may bias concentration estimates, eg, in studies with cohort differences in metabolite T_2 relaxation,[44] the use of the SPECIAL or sSPECIAL sequence with a T_E < 20 ms is recommended. However, these populations may also be more prone to motion. Therefore, when a T_E < 20 ms is important and SPECIAL leads to unacceptable motion artefacts, the use of the single-shot STEAM sequence is recommended if the SNR of individual transients is sufficient for frequency and phase correction. In these cases, we recommend using a version of the STEAM sequence with ultrashort T_E (<10 ms) and an optimized water suppression and gradient scheme for efficient unwanted coherence removal[13]; product sequences on some platforms only allow a minimum T_E of 20 ms (Table 1) and have not been optimized to provide artifact-free single shots. Also, note that although short T_E values, and typically 30 ms, are recommended for quantification of metabolite profiles, longer T_Es may be preferred for select metabolites.[2]

The sLASER and sSPECIAL sequences reduce CSDE to below the recently recommended 4% per ppm level[2] at 3 T in all three dimensions, while the original version of SPECIAL exceeds this value along the refocusing dimension (Table 1). At 7 T, very high B_1^+(max) levels (~ 35-45 μT) are needed to achieve sufficiently broad bandwidths using conventional pulses (both for excitation and adiabatic refocusing, eg, with hyperbolic secant pulses) to stay within a 4% ppm CSDE at short T_E. Therefore, we recommend the use of gradient-modulated adiabatic RF pulses[45] such as FOCI and GOIA to reduce B_1^+ requirements[26] and allow adiabatic refocusing at short T_E within the 4% per ppm CSDE limit at 7 T with commercially available head RF coils that can deliver ~ 24-26 μT. Note, however, that in the localization direction of the excitation pulse, the recommended 4% per ppm CSDE limit cannot yet be reached for short T_E MRS with commercial volume coils at 7 T and that current implementations remain at 7% per ppm CSDE in this dimension (Table 1).

Finally, to overcome the inhomogeneous B_1^+ fields in applications in the torso, gradient-modulated adiabatic RF pulses are recommended to generate sufficient bandwidth at low B_1^+ while keeping the CSDE to acceptable levels at both 3 and 7 T.[45-48] Note, however, that the off-resonance effects of these pulses need to be evaluated for optimum pulse selection since the effects can be high, particularly in body applications.[45]

These sequences are available through research packages directly from the manufacturer (designated work-in-progress [WIP] at Siemens and GE) or through customer-to-customer sequence exchange protocols for Siemens, GE and Philips platforms. A list of the currently available sources for the localization sequences is provided in Table S2.

4.3 | Recommendations for data acquisition: QA

4.3.1 | VOI selection

Manual VOI prescription is an important source of variability in SVS protocols. We recommend the use of commercially available tools to minimize this variability across subjects and scan sessions. For example, the AutoAlign tool on Siemens (currently available for brain, spine, knee, shoulder and hip acquisitions),[49] and the SmartExam tool on Philips (currently available for brain, spine, knee and shoulder acquisitions),[50] align scout images of a subject to predefined landmarks or an average atlas and facilitate the acquisition of subsequent images in a uniform space. These tools are particularly useful to ensure consistency of VOI selection in longitudinal scans of the same subject.[51] In addition, atlas-based automatic voxel positioning to improve VOI consistency both between and within subjects has recently been implemented for SVS in the brain,[52] but is only available at selected research sites.[26] In muscle SVS, the interplay between dipolar coupling and orientation of the muscle with respect to the B_0 direction needs to be considered when choosing VOI size and location.

4.3.2 | B_0 adjustment

Methods to adjust both first- and second-order shims for the targeted VOI using fully automated B_0 field mapping techniques, either based on 3D B_0 mapping or mapping along projections, are recommended for use within advanced MRS protocols at high fields. For a detailed review of advanced methods for B_0 shimming, as well as currently available B_0 shimming tools (vendor-provided and through customer-to-customer exchange protocols), we refer the reader to another contribution in this special issue.[33]

Commercial B_0 shimming protocols for first- and second-order shim adjustments are continually improving on 3 and 7 T systems and they provide acceptable linewidths (see section 4.3.4) for most VOIs in the brain. In addition, the FASTMAP[53] technique based on mapping along projections was incorporated into the sLASER sequence for automatic VOI-based B_0 shimming and is available via customer-to-customer sequence exchange for one of the platforms (Table S2).

Creating a sufficiently homogeneous B_0 within the VOI is more challenging in the body. Especially when lipids are present (eg, in a voxel in breast tissue or fatty infiltrated muscle), shimming needs to be performed only on the water signal by either water-selective excitation or lipid suppression in the B_0 shimming algorithm. Following shimming, the correct carrier frequency (F_0) needs to be determined for the VOI. Depending on the MR system software, this can be carried out by volume-selective excitation and interactively choosing the correct resonance peak of water or by adding an inversion pulse to the automated F_0 determination with a delay which corresponds to fat nulling. In the presence of motion, a navigator is recommended to enable triggering of the volume-selective F_0 determination.

4.3.3 | B_1 adjustment

To prevent incorrect flip angle calibration for SVS acquisition, VOI-based flip angle calibration is strongly recommended at 3 T and higher for accurate localization. The consequences of B_1 miscalibration on RF pulse profiles that result in excitation of unintended magnetization and ineffective refocusing are demonstrated in Figure 2. Importantly, the B_1 levels in the VOI can be underestimated or overestimated in close to half of the MRS datasets with slice-based RF power calibration typically used during the system prescan protocol compared with B_1 levels calibrated in the VOI. VOI-based B_1 calibration is standard in advanced MRS techniques distributed via WIP or customer-to-customer sequence exchange, but may require some user intervention, eg, acquiring the water signal from the VOI with increasing RF power and choosing the power setting which produces the maximum signal. Similar to flip angle calibration in product sequences, automated VOI-based flip angle calibration is available for sLASER on some platforms (Table S2). As mentioned earlier, for body applications at 7 T, a multichannel transmit coil and local B_1^+ shimming are essential for optimal RF delivery.

4.3.4 | Selection of acquisition parameters and QA decisions during data acquisition

Once the pulse sequence and associated parameters are optimized, as in the advanced sequences available via WIP or customer-to-customer sequence exchange (Table S2), the MR operator should not need to manually adjust any sequence parameters (eg, timing, selection of OVS bands) during each scanning session and can proceed with data acquisition following voxel-based B_0 and B_1 adjustments. Furthermore, once a protocol is chosen for a research study or a particular clinical evaluation, any adjustment of parameters such as T_R and T_E should be strictly avoided to enable comparison of quantitative data between subjects, cohorts and sites.

Acquisition of unsuppressed water signal from the same VOI is strongly recommended for the purposes of eddy current correction, quantification and RF coil combination.[54] The water signal should be acquired with the same gradients as the metabolite spectrum to enable eddy current correction based on the reference water spectrum.[55] When the water reference is used as a quantification reference, the OVS pulses should be turned off to prevent magnetization transfer (MT) effects from the OVS. While turning off the OVS pulses for the water signal acquisition may

result in a slight underestimation of concentrations, this effect is substantially smaller than the MT effects observed with the OVS pulses left on, which may result in up to ~ 30% overestimation of concentrations depending on VOI location.[17] The carrier frequency for the water acquisition should be set to the water resonance. Finally, the unsuppressed water signal should be acquired before the metabolite spectrum to ensure that a water reference from the correct VOI is available if the metabolite acquisition needs to be stopped due to a change in subject position, and such that partially acquired metabolite data can be quantified using the correct water reference.

For both the water and metabolite acquisitions, individual shots, and not only the summed data, should be saved such that minor motion effects and frequency drifts can be corrected during preprocessing. The MR operator should evaluate water suppression efficiency, spectral linewidth and SNR at the beginning and during the MRS acquisition to address any unexpected deterioration in data quality over time. A change in the subject position may be indicated by a change in linewidth, frequency and/or spectral pattern, as well as worsening of water suppression. If there is indication of a change in subject position from the MRS acquisition, a scout image should be acquired after MRS to confirm the change in position.

Preferably, the residual water signal needs to be below or at the same height as the largest metabolite peak. Minimally, the tail of the residual water peak should not affect the spectral baseline. If very small VOIs are studied and single shots do not contain clear metabolite peaks, some residual water signal may be desirable to allow single-shot frequency and phase alignment. The spectral linewidth should be evaluated with an unsuppressed water acquisition from the same VOI prior to commencing with metabolite acquisition. At 3 T, a water linewidth of 5-7 Hz (full width at half maximum determined in a phased spectrum) is considered excellent, 8-10 Hz is considered good and 11-13 Hz acceptable for brain applications. At 7 T, these ranges are 9-12 Hz (excellent), 13-15 Hz (good) and 16-19 Hz (acceptable), but note that the best achievable linewidths depend on the VOI location.[33] The reader is referred to another contribution in this special issue concerning recommendations on linewidths for all brain and body applications at field strengths from 1.5-7 T.[33] Also, note that if the VOI contains a substantial amount of cerebrospinal fluid in brain acquisitions, the linewidth of the water signal will be smaller than that of pure tissue water and therefore will not accurately reflect the linewidth of the metabolite spectrum that originates from the tissue in the VOI. Finally, a minimum SNR, defined as the largest peak height divided by the standard deviation of noise measured in a metabolite-free region of the spectrum, of ~ 3 in single shots, is recommended to allow for frequency and phase alignment during preprocessing.

4.3.5 | Mitigation of motion artifacts

At a minimum, phase and frequency variations should be corrected retrospectively in single shots.[56-58] In addition, prospective motion correction strategies are highly recommended. Prospectively gated acquisitions[59] are relatively easy to implement and have the advantage of confining the volume of acquisition more precisely to the prescribed volume, but are constrained to use a relatively long T_R. Whenever available, prospective volume tracking methods should be used,[60-62] ideally in conjunction with dynamic linear shim corrections,[63] because even when the VOI position is updated in real time, the spectral quality can degrade substantially without dynamic shim updates.[64]

4.4 | Recommendations for data analysis: QC

An in-depth discussion of MRS preprocessing and spectral analysis steps is presented in another paper in this special issue.[54] Here, we emphasize the critical considerations for analysis of data acquired using advanced SVS methodology.

Spectral quality is often determined primarily by the localization performance of the pulse sequence and by the capability of the B_0 shim system to remove a spatial B_0 inhomogeneity within the selected VOI. However, the quality of the resulting averaged spectrum can be degraded by frequency and phase variations caused by physiological motion and scanner drift (eg, subsequent to fast imaging acquisitions). These fluctuations should be corrected by aligning the frequency and phase of single shots in preprocessing. If single shots do not have sufficient SNR to allow frequency and phase alignment, some averaging prior to alignment is acceptable. In addition, uncorrectable spectra due to substantial motion, eg, those with very large residual water, unwanted coherences or substantially broader linewidth than other transients in the same acquisition, should be excluded from averaging. These outliers can either be identified by visual inspection or by unsupervised outlier detection.[54] Following averaging, residual eddy current effects should be eliminated using the unsuppressed water signal.[55]

The final spectra should be evaluated for spectral linewidths, SNR, efficiency of water suppression and presence of unwanted coherences. The criteria for acceptable linewidths and water suppression are the same as those listed in section 4.3.4. In addition, residual water can be effectively removed[54] using tools such as the Hankel Lanczos singular value decomposition method. A minimum metabolite SNR of 3 was previously recommended to visually confirm the presence of a particular singlet.[2] When using advanced MRS protocols, we recommend a minimum SNR of 3 in individual transients to enable frequency and phase corrections in single shots prior to averaging. Substantially higher SNR levels are necessary for reliable metabolite profile quantification and are readily achieved in summed spectra obtained from VOI of $\geq$ ~ 4 mL in the brain using advanced MRS protocols at 3 and 7 T. The spectral pattern of macromolecules ~ 1.5 ppm for brain and lipid signals for body applications should be compared with the expected patterns of macromolecule and lipid signals to evaluate if there is contamination by signals of subcutaneous lipids originating outside the VOI. In addition, unwanted coherences should be evaluated in the entire ppm range of the spectrum that will be used for quantification. Unwanted coherences, also termed spurious echoes, typically appear as high frequency signals and/or signals that are out of phase

with the rest of the spectrum. Examples are presented in a separate contribution in this special issue.[54] Spectra that do not fit the linewidth and water suppression quality criteria and those with substantial unwanted coherence contamination[65] should be excluded from analysis.

Software packages that allow single shot frequency/phase and eddy current corrections and evaluation of averaged spectra are available to the MRS community.[57,66-68]

Averaged spectra should be fitted using automated parametric fitting packages[69,70] with a basis set generated for the parameters used for data acquisition. For brain spectra, macromolecules should be accounted for during parametric fitting,[71] ideally by using an experimentally measured macromolecule basis spectrum since mathematically estimated macromolecules introduce biases in the quantification of J-coupled and low concentration metabolites.[7,72] To acquire data for a macromolecular basis spectrum, typically an inversion pulse is added to the pulse sequence to null the signals from metabolites and the inversion time is field-dependent. For more details on how to acquire the macromolecule basis spectrum, the reader is referred to the paper in this special issue focusing on the contribution of macromolecules to spectra.[71] In addition, advanced sequences that have macromolecule acquisition capability are indicated in Table S2.

Criteria for determining the reliability of concentration measurements should be based on quantitative error estimates such as CRLB. When selecting the CRLB criteria for evaluating the reliability of metabolite concentrations, potential biases in the estimated mean concentrations of cohort data should be considered when CRLB thresholds are used to filter metabolite concentrations.[37] For instance, relative CRLB higher than 50% indicate that the metabolite concentration may be anywhere from zero to twice the estimated concentration. Therefore, in some studies, all concentrations that have CRLB higher than 50% or another chosen threshold are excluded. However, this approach will not yield the mean concentration of the larger cohort, rather it will yield the mean value of the subset of data which agree with each other within the cohort.[37] On the other hand, a high relative CRLB may indicate that a metabolite is not detectable in an individual spectrum, which may be biologically significant when a diagnostic decision needs to be made with a single spectrum. To define which metabolites can be evaluated reliably under the conditions of the study, a CRLB threshold can be selected to exclude metabolites with average CRLB above the threshold (with the mean CRLB calculated without filtering) or to exclude metabolites with CRLB above the threshold in the majority of cases. In cohort comparison studies, this process should be undertaken in both groups separately (eg, patient, control) to keep the metabolites that pass the reliability threshold in either cohort, and not to miss metabolites that may be substantially lower in one group than the other, with important biological meaning. Finally, for low metabolite concentrations, an absolute, rather than relative, CRLB threshold can be chosen to avoid the bias of removing smaller concentration values.

4.5 | Recommendations for the reporting of advanced SVS data

Reporting guidelines for MRS studies are detailed in another paper in this special issue.[73] Here, we would like to reiterate the importance of always providing information on the field strength and RF coil, acquisition parameters (sequence used, T_R, T_E, number of transients, total acquisition time, number of points, bandwidth of the RF pulses and CSDE, VOI location and size), average SNR and linewidth (of associated water reference and/or metabolites), fitting parameters (fitting software and version, metabolites included in the basis set, handling of macromolecules and baseline, tissue water content used for referencing) and outcomes (CRLB of fitted metabolites, reliability criteria used) to enable proper comparison of findings between studies. Sample MR spectra should always be included, ideally together with images that show the VOI position. For these sample spectra, authors should consider reporting their spectral quality parameters (SNR, linewidth, CRLB if quantification results are reported) to place them in the context of all spectra acquired in the project. Alternatively, mean and standard deviation of spectra from each studied cohort can be reported for a more complete representation of spectral quality in the study. Spectra can be supplied in an appendix or as supporting information if space for figures is limited. Finally, cohort comparison studies should evaluate spectral quality differences between cohorts and address potential biases if differences are found.

5 | RECOMMENDATIONS FOR MR SCANNER VENDORS

5.1 | Hardware

Even although the latest high-field scanners from all major MRI vendors meet the basic hardware requirements for ^{1}H MRS, spectroscopy acquisitions place high demands on the RF transmit system (RF amplifiers, RF coils) and the second-order shim system for adjustment of the B_0 field homogeneity.[32] The maximum available transmit B_1^+ field is a key variable affecting the localization performance of MRS techniques (CSDE, minimum T_E). The B_1^+(max) of 13-25 µT provided by the built-in body transmit RF coils of 3 T scanners is sufficient for a T_E of 30 ms or less in SPECIAL and sLASER for brain acquisitions (Table 1).[26] The B_1 demands are substantially higher at 7 T, both for brain and body applications. We encourage vendors to provide commercial multielement transmit/receive arrays and B_1^+ shimming capability to 7 T users,[41] similar to those that were used in the research setting to achieve B_1^+ levels of ~ 35 µT.[42]

Second-order shim systems currently available on 3 T scanners are sufficient to obtain high quality SVS data in most regions. For regions with large B_0 inhomogeneities, such as the hippocampus, prefrontal cortex or the brainstem, and for body applications, stronger second-order shim coils are desirable. The strength of the second-order shims on human 7 T scanners should be at least 30 Hz/cm^2 (0.7 mT/cm^2) for XZ, YZ and Z2 and 15 Hz/cm^2 (0.3 mT/cm^2) for XY and X2Y2 shims.[13,32]

5.2 | Scanner software

First and foremost we urge vendors to provide advanced, optimized MRS acquisition protocols as part of the commercial MRS packages approved by the US Food and Drug Administration (FDA) or the European Medicines Agency (EMA). While these protocols are available to the community via WIP or customer-to-customer sequence exchange, support for these packages at the level of a commercial package by any research laboratory is challenging and not optimally sustainable, especially with frequent software updates implemented by vendors. In these advanced protocols, user intervention should be minimized by automating voxel-based B_0 and B_1 adjustments and VOI selection for applications where a predefined VOI has to be used in the same location across subjects. We further encourage vendors to enable users to evaluate sequence performance, eg, by visualizing VOI profiles, and to implement tools to measure linewidth and SNR on the scanner. Importantly, FDA/EMA-approved tools for in-line quantification for MR spectra, including quantitative error estimates, are strongly recommended.[1] As multielement receive array coils have become standard for 3 and 7 T scanners, we recommend automatic collection of a water reference in the same acquisition as the metabolites for effective RF coil combination based on the water signal. Finally, implementation of methods that enable prospective volume tracking and dynamic linear shim corrections are strongly recommended to improve both MRS and MRI data quality and to prevent substantial loss of scanner time due to repeated acquisitions.

An important challenge for multisite trials is to ensure harmonization of advanced SVS methods if metabolite levels are to be used as outcome measures. The feasibility of pooling neurochemical profiles obtained on different 3 T scanners from the same vendor was demonstrated,[74] as well
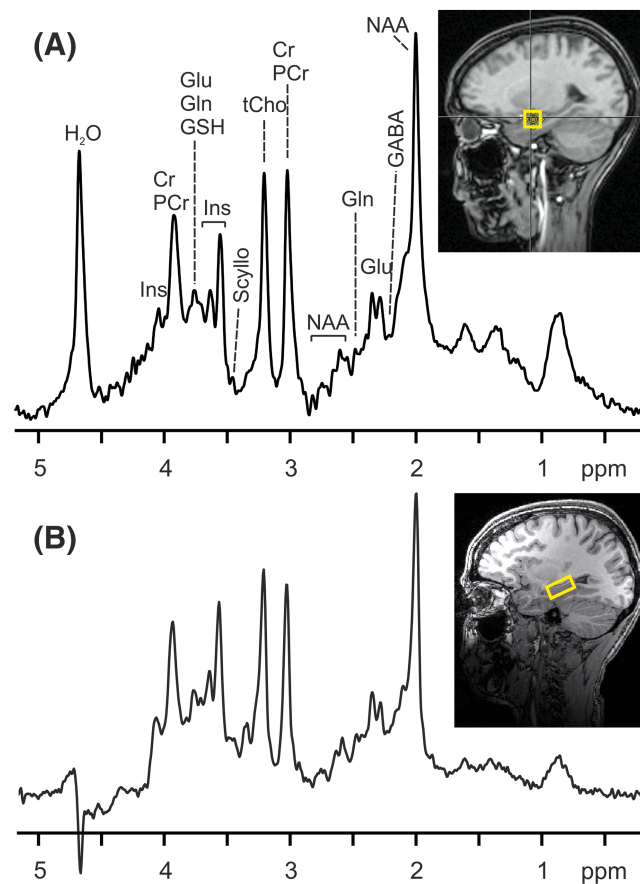
FIGURE 5 (A) ^{1}H MR spectrum acquired from the amygdala of a healthy volunteer at 3 T with the SPECIAL sequence: volume of interest (VOI) = 15 x 15 x 15 mm^3, T_R/T_E = 3000/6 ms, number of transients (NT) = 256, T_{acq} = 1024 ms and number of points = 2048. (B) ^{1}H MR spectrum acquired from the hippocampus of a healthy volunteer at 3 T with the semiadiabatic LASER (sLASER) sequence: VOI = 13 x 26 x 12 mm^3, T_R/T_E = 5000/28 ms, NT = 128, T_{acq} = 341 ms and number of points = 2048. Data processing consisted of zero-filling up to 8-k data points, Gaussian multiplication of the FID (σ = 0.28/second), Fourier transformation and phase correction. Insets: sagittal T_1-weighted images with the location of the VOI

as the feasibility of replicating an sLASER protocol across vendors.[26,43] To enable pooling MRS data obtained in multisite clinical trials, we encourage vendors to implement comparable acquisition sequences, shimming hardware and software, data format and storage protocols, and options to display CSDE and to adjust gradient and chemical shift directions in MRS sequences. Ideally, at least one advanced SVS sequence that maintains cross-vendor equivalence of sequence RF and gradients should be maintained as already established within the MRS community.

6 | SUCCESSFUL APPLICATIONS OF ADVANCED SVS AND CONCLUSIONS

Advanced MRS methods allow reproducible quantification of a neurochemical profile at 3 T, even in challenging VOIs that have not been feasible to study with conventional SVS methods, but are of high interest for neuroscience and clinical applications, such as the hippocampus[35] and amygdala (Figure 5).[29] Furthermore, the sLASER prelocalization technique for MRSI can provide high quality data in the body leading to reproducible biomarkers in oncology, such as the (tCho+PA+Cr)/Cit in prostate cancer.[75] In addition, sLASER enabled 2-hydroxyglutarate detection in the brain, which is a biomarker for IDH-1 mutations in glial brain tumors, as well as differentiation of tumors with IDH1 from those with IDH2 mutations.[76] In neurologic diseases, advanced MRS protocols at high field have allowed the detection of subtle metabolite differences between patient and control groups,[77] including at very early and premanifest stages,[78] and have helped to monitor treatment response.[79] Advanced MRS has also been used in drug discovery applications in psychiatric disorders.[80] In metabolic diseases, advanced SVS methods have allowed dynamic measurements of glucose and its catabolic products.[81,82] Finally, advanced MRS protocols have enabled reliable detection of subtle brain metabolite responses to visual,[83] cognitive[84] and motor[85] stimuli. Taken together, these examples show that advanced MRS sequences with optimized acquisition and data analysis protocols, such as those recommended in this paper, have added value in clinical diagnostics and research. With their increasing availability, especially if implemented as product sequences, they are expected to substantially increase the data quality achievable by MRS in the clinical setting and thereby contribute to the wider utility and use of the technology.

ABBREVIATIONS USED

AFP	adiabatic full passage
B_1^+	transmit B_1
Cho	choline
Cit	citrate
Cr	creatine
CRLB	Cramér-Rao lower bound
CSDE	chemical shift displacement error
CV	coefficient of variance
FASTMAP	fast automatic shimming technique by mapping along projections
FID	free induction decay
FOCI	frequency offset corrected inversion
FOV	field of view
GABA	γ–aminobutyric acid
Glx	glutamate + glutamine
GOIA	gradient offset independent adiabatic
IDH	isocitrate dehydrogenase
ISIS	image-selected in vivo spectroscopy
LASER	localization by adiabatic selective refocusing
OVS	outer volume suppression
PRESS	point-resolved spectroscopy
^{1}H MRS	proton MR spectroscopy
QA	quality assurance
QC	quality control
RF	radiofrequency

SAR   specific absorption rate

sLASER   semiadiabatic LASER

SNR   signal-to-noise ratio

SPECIAL   spin echo full intensity acquired localized spectroscopy

sSPECIAL   semiadiabatic SPECIAL

STEAM   stimulated echo acquisition mode

SVS   single voxel spectroscopy

tCho   total choline (glycerophosphocholine + phosphocholine + choline)

tCr   total creatine (creatine + phosphocreatine)

tNAA   total *N*-acetylaspartate (*N*-acetylaspartate + *N*-acetylaspartylglutamate)

VAPOR   variable pulse power and optimized relaxation delays

VOI   volume of interest

WIP   work-in-progress

ORCID

Gülin Öz https://orcid.org/0000-0002-5769-183X

Dinesh K. Deelchand https://orcid.org/0000-0003-4266-4780

Lijing Xin https://orcid.org/0000-0002-5450-6109

REFERENCES

1. Öz G, Alger JR, Barker PB, et al. Clinical proton MR spectroscopy in central nervous system disorders. *Radiology*. 2014;270(3):658-679.

2. Wilson M, Andronesi OC, Alger JR, et al. A Methodological consensus on clinical proton MR spectroscopy of the brain: review and recommendations. *Magn Reson Med*. 2019;82(2):527-550.

3. Choi IY ,et al. Spectral editing in ^{1}H magnetic resonance spectroscopy: Experts' consensus recommendations. *NMR Biomed*. 2020.

4. Lange T, Dydak U, Roberts TP, Rowley HA, Bjeljac M, Boesiger P. Pitfalls in lactate measurements at 3T. *Ajnr*. 2006;27(4):895-901.

5. Vaughan JT, Garwood M, Collins CM, et al. 7T vs. 4T: RF power, homogeneity, and signal-to-noise comparison in head images. *Magn Reson Med*. 2001;46(1):24-30.

6. Balchandani P, Naidich TP. Ultra-high-field MR neuroimaging. *Ajnr*. 2015;36(7):1204-1215.

7. Deelchand DK, Kantarci K, Öz G. Improved localization, spectral quality, and repeatability with advanced MRS methodology in the clinical setting. *Magn Reson Med*. 2018;79(3):1241-1250.

8. Koch KM, Rothman DL, de Graaf RA. Optimization of static magnetic field homogeneity in the human and animal brain in vivo. *Prog NMR Spect*. 2009;54:69-96.

9. Frahm J, Merboldt K-D, Hänicke W. Localized proton spectroscopy using stimulated echoes. *J Magn Reson*. 1987;72(3):502-508.

10. Bottomley PA, inventor. Selective volume method for performing localized NMR spectroscopy. US patent 4 480 228, 1984.

11. Ordidge RJ, Bendall MR, Gordon RE, Connelly A. Volume selection for in vivo biological spectroscopy. In: Govil G, Khetrapal CL, Saran A, eds. *Magnetic Resonance in Biology and Medicine*. New Delhi, India: McGraw Hill; 1985:387-397.

12. Mlynárik V, Gambarota G, Frenkel H, Gruetter R. Localized short-echo-time proton MR spectroscopy with full signal-intensity acquisition. *Magn Reson Med*. 2006;56(5):965-970.

13. Tkáč I, Gruetter R. Methodology of ^{1}H NMR Spectroscopy of the human brain at very high magnetic fields. *Appl Magn Reson*. 2005;29:139-157.

14. Slotboom J, Mehlkopf AF, Bovée WMMJ. A single-shot localization pulse sequence suited for coils with inhomogeneous RF fields using adiabatic slice-selective RF pulses. *J Magn Reson*. 1991;95(2):396-404.

15. Garwood M, DelaBarre L. The return of the frequency sweep: designing adiabatic pulses for contemporary NMR. *J Magn Reson*. 2001;153(2):155-177.

16. Scheenen TW, Klomp DW, Wijnen JP, Heerschap A. Short echo time ^{1}H-MRSI of the human brain at 3T with minimal chemical shift displacement errors using adiabatic refocusing pulses. *Magn Reson Med*. 2008;59(1):1-6.

17. Öz G, Tkáč I. Short-echo, single-shot, full-intensity proton magnetic resonance spectroscopy for neurochemical profiling at 4 T: validation in the cerebellum and brainstem. *Magn Reson Med*. 2011;65(4):901-910.

18. Marjańska M, Auerbach EJ, Valabregue R, Van de Moortele PF, Adriany G, Garwood M. Localized ^{1}H NMR spectroscopy in different regions of human brain in vivo at 7 T: T_2 relaxation times and concentrations of cerebral metabolites. *NMR Biomed*. 2012;25(2):332-339.

19. Boer VO, van Lier AL, Hoogduin JM, Wijnen JP, Luijten PR, Klomp DW. 7-T ^{1}H MRS with adiabatic refocusing at short TE using radiofrequency focusing with a dual-channel volume transmit coil. *NMR Biomed*. 2011;24(9):1038-1046.

20. Tkáč I, Starcuk Z, Choi I-Y, Gruetter R. In vivo ^{1}H NMR spectroscopy of rat brain at 1 ms echo time. *Magn Reson Med*. 1999;41:649-656.

21. Carr HY, Purcell EM. Effects of diffusion on free precession in nuclear magnetic resonance experiments. *Phys Rev*. 1954;94(3):630-638.

22. Deelchand DK, Henry P-G, Marjańska M. Effect of Carr-Purcell refocusing pulse trains on transverse relaxation times of metabolites in rat brain at 9.4 Tesla. *Magn Reson Med*. 2015;73(1):13-20.

23. Michaeli S, Garwood M, Zhu XH, et al. Proton T_2 relaxation study of water, N-acetylaspartate, and creatine in human brain using Hahn and Carr-Purcell spin echoes at 4T and 7T. *Magn Reson Med*. 2002;47(4):629-633.

24. Ordidge RJ, Wylezinska M, Hugg JW, Butterworth E, Franconi F. Frequency offset corrected inversion (FOCI) pulses for use in localized spectroscopy. *Magn Reson Med*. 1996;36(4):562-566.

25. Tannus A, Garwood M. Adiabatic pulses. *NMR Biomed*. 1997;10(8):423-434.

26. Deelchand D, Berrington A, Noeske R, et al. Across-vendor standardization of semi-LASER for single-voxel MRS at 3 Tesla. *NMR Biomed*. 2019. https://onlinelibrary.wiley.com/doi/abs/10.1002/nbm.4218

27. Ordidge RJ, Connelly A, Lohman JAB. Image-selected in vivo spectroscopy (ISIS). A new technique for spatially selective nmr spectroscopy. *J Magn Reson*. 1986;66(2):283-294.

28. Mekle R, Mlynárik V, Gambarota G, Hergt M, Krueger G, Gruetter R. MR spectroscopy of the human brain with enhanced signal intensity at ultrashort echo times on a clinical platform at 3T and 7T. *Magn Reson Med*. 2009;61(6):1279-1285.

29. Schubert F, Kuhn S, Gallinat J, Mekle R, Ittermann B. Towards a neurochemical profile of the amygdala using short-TE ^{1}H magnetic resonance spectroscopy at 3 T. *NMR Biomed*. 2017;30(5):e3685. https://onlinelibrary.wiley.com/doi/abs/10.1002/nbm.3685

30. Fuchs A, Luttje M, Boesiger P, Henning A. SPECIAL semi-LASER with lipid artifact compensation for ^{1}H MRS at 7 T. *Magn Reson Med*. 2013;69(3):603-612.

31. Xin L, Schaller B, Mlynárik V, Lu H, Gruetter R. Proton T_1 relaxation times of metabolites in human occipital white and gray matter at 7 T. *Magn Reson Med*. 2013;69(4):931-936.

32. Xin L, Tkáč I. A practical guide to in vivo proton magnetic resonance spectroscopy at high magnetic fields. *Anal Biochem*. 2017;529:30-39.

33. Juchem C, et al. B0 shimming techniques: Experts' consensus recommendations. *NMR Biomed*. 2020.

34. Terpstra M, Cheong I, Lyu T, et al. Test-retest reproducibility of neurochemical profiles with short-echo, single-voxel MR spectroscopy at 3T and 7T. *Magn Reson Med*. 2016;76(4):1083-1091.

35. Bednarik P, Moheet A, Deelchand DK, et al. Feasibility and reproducibility of neurochemical profile quantification in the human hippocampus at 3 T. *NMR Biomed*. 2015;28(6):685-693.

36. Wijnen JP, van Asten JJ, Klomp DW, et al. Short echo time ^{1}H MRSI of the human brain at 3T with adiabatic slice-selective refocusing pulses; reproducibility and variance in a dual center setting. *J Magn Reson Imaging*. 2010;31(1):61-70.

37. Kreis R. The trouble with quality filtering based on relative Cramer-Rao lower bounds. *Magn Reson Med*. 2015;75(1):15-18.

38. Lemke C, Hess A, Clare S, et al. Two-voxel spectroscopy with dynamic B0 shimming and flip angle adjustment at 7 T in the human motor cortex. *NMR Biomed*. 2015;28(7):852-860.

39. Snaar JE, Teeuwisse WM, Versluis MJ, et al. Improvements in high-field localized MRS of the medial temporal lobe in humans using new deformable high-dielectric materials. *NMR Biomed*. 2011;24(7):873-879.

40. Tkáč I, Andersen P, Adriany G, Merkle H, Ugurbil K, Gruetter R. In vivo ^{1}H NMR spectroscopy of the human brain at 7 T. *Magn Reson Med*. 2001;46(3):451-456.

41. Van de Moortele PF, Akgun C, Adriany G, et al. B(1) destructive interferences and spatial phase patterns at 7 T with a head transceiver array coil. *Magn Reson Med*. 2005;54(6):1503-1518.

42. Emir UE, Auerbach EJ, Moortele PF, et al. Regional neurochemical profiles in the human brain measured by ^{1}H MRS at 7 T using local B1 shimming. *NMR Biomed*. 2012;25(1):152-160.

43. van de Bank BL, Emir UE, Boer VO, et al. Multi-center reproducibility of neurochemical profiles in the human brain at 7 T. *NMR Biomed*. 2015;28(3):306-316.

44. Marjańska M, Emir UE, Deelchand DK, Terpstra M. Faster metabolite ^{1}H transverse relaxation in the elder human brain. *PLoS ONE*. 2013;8(10):e77572. https://www.ncbi.nlm.nih.gov/pubmed/24098589

45. Andronesi OC, Ramadan S, Ratai EM, Jennings D, Mountford CE, Sorensen AG. Spectroscopic imaging with improved gradient modulated constant adiabaticity pulses on high-field clinical scanners. *J Magn Reson*. 2010;203(2):283-293.

46. Arteaga de Castro CS, Boer VO, Andreychenko A, et al. Improved efficiency on editing MRS of lactate and gamma-aminobutyric acid by inclusion of frequency offset corrected inversion pulses at high fields. *NMR Biomed*. 2013;26(10):1213-1219.

47. Payne GS, Leach MO. Implementation and evaluation of frequency offset corrected inversion (FOCI) pulses on a clinical MR system. *Magn Reson Med*. 1997;38(5):828-833.

48. Steinseifer IK, van Asten JJ, Weiland E, Scheenen TW, Maas MC, Heerschap A. Improved volume selective ^{1}H MR spectroscopic imaging of the prostate with gradient offset independent adiabaticity pulses at 3 Tesla. *Magn Reson Med*. 2015;74(4):915-924.

49. van der Kouwe AJ, Benner T, Fischl B, et al. On-line automatic slice positioning for brain MR imaging. *Neuroimage*. 2005;27(1):222-230.

50. Young S, Bystrov D, Netsch T, et al. Automated planning of MRI neuro scans. *Proc SPIE*. 2006;6144:1–861441M.

51. Dou W, Speck O, Benner T, et al. Automatic voxel positioning for MRS at 7 T. *MAGMA*. 2015;28(3):259-270.

52. Park YW, Deelchand DK, Joers JM, et al. AutoVOI: real-time automatic prescription of volume-of-interest for single voxel spectroscopy. *Magn Reson Med*. 2018;80(5):1787-1798.

53. Gruetter R, Tkáč I. Field mapping without reference scan using asymmetric echo-planar techniques. *Magn Reson Med*. 2000;43(2):319-323.

54. Near J, Harris AD, Juchem C, et al. Preprocessing, analysis and quantification in single-voxel magnetic resonance spectroscopy: Experts' consensus recommendations. *NMR Biomed*. 2020.

55. Klose U. In vivo proton spectroscopy in presence of eddy currents. *Magn Reson Med*. 1990;14(1):26-30.

56. Öz G, Tkáč I, Charnas LR, et al. Assessment of adrenoleukodystrophy lesions by high field MRS in non-sedated pediatric patients. *Neurology*. 2005;64(3):434-441.

57. Near J, Edden R, Evans CJ, Paquin R, Harris A, Jezzard P. Frequency and phase drift correction of magnetic resonance spectroscopy data by spectral registration in the time domain. *Magn Reson Med*. 2015;73(1):44-50.

58. Noworolski SM, Tien PC, Merriman R, Vigneron DB, Qayyum A. Respiratory motion-corrected proton magnetic resonance spectroscopy of the liver. *Magn Reson Imaging*. 2009;27(4):570-576.

59. Weis J, Kullberg J, Ahlstrom H. Multiple breath-hold proton spectroscopy of human liver at 3T: Relaxation times and concentrations of glycogen, choline, and lipids. *J Magn Reson Imaging*. 2018;47(2):410-417.

60. Andronesi OC ,et al. Frequency and motion correction techniques for magnetic resonance spectroscopy: Experts' consensus recommendations. *NMR Biomed*. 2020.

61. Zaitsev M, Speck O, Hennig J, Buchert M. Single-voxel MRS with prospective motion correction and retrospective frequency correction. *NMR Biomed*. 2010;23(3):325-332.

62. Kozerke S, Schar M, Lamb HJ, Boesiger P. Volume tracking cardiac 31P spectroscopy. *Magn Reson Med*. 2002;48(2):380-384.

63. Keating B, Ernst T. Real-time dynamic frequency and shim correction for single-voxel magnetic resonance spectroscopy. *Magn Reson Med*. 2012;68(5):1339-1345.

64. Deelchand DK, Joers JM, Auerbach EJ, Henry PG. Prospective motion and B0 shim correction for MR spectroscopy in human brain at 7T. *Magn Reson Med*. 2019;82(6):1984-1992.

65. Kreis R. Issues of spectral quality in clinical 1H-magnetic resonance spectroscopy and a gallery of artifacts. *NMR Biomed*. 2004;17(6):361-381.

66. MRspa: Magnetic Resonance signal processing and analysis. 2019. https://www.cmrr.umn.edu/downloads/mrspa/. Accessed date December 2, 2019.

67. VeSPA - Versatile Simulation, Pulses, and Analysis. 2019. https://scion.duhs.duke.edu/vespa/. Accessed date December 2, 2019.

68. Juchem C. INSPECTOR - Magnetic Resonance Spectroscopy Software. Columbia TechVenture (CTV): p. License CU17130; 2016.

69. Poullet JB, Sima DM, Van Huffel S. MRS signal quantitation: a review of time- and frequency-domain methods. *J Magn Reson*. 2008;195(2):134-144.

70. Graveron-Demilly D. Quantification in magnetic resonance spectroscopy based on semi-parametric approaches. *MAGMA*. 2014;27(2):113-130.

71. Cudalbu C ,et al. Contribution of macromolecules to magnetic resonance spectra: Experts' consensus recommendations. *NMR Biomed*. 2020.

72. Schaller B, Xin L, Cudalbu C, Gruetter R. Quantification of the neurochemical profile using simulated macromolecule resonances at 3 T. *NMR Biomed*. 2013;26(5):593-599.

73. Lin A ,et al. Reporting guidelines for magnetic resonance spectroscopy publications: Experts' consensus recommendations. *NMR Biomed*. 2020.

74. Deelchand DK, Adanyeguh IM, Emir UE, et al. Two-site reproducibility of cerebellar and brainstem neurochemical profiles with short-echo, single voxel MRS at 3 T. *Magn Reson Med*. 2015;73(5):1718-1725.

75. Tayari N, Steinseifer IK, Selnaes KM, Bathen TF, Maas MC, Heerschap A. High-quality 3-dimensional 1H magnetic resonance spectroscopic imaging of the prostate without endorectal receive coil using a semi-LASER sequence. *Invest Radiol*. 2017;52(10):640-646.

76. Emir UE, Larkin SJ, de Pennington N, et al. Noninvasive quantification of 2-hydroxyglutarate in human gliomas with IDH1 and IDH2 mutations. *Cancer Res*. 2016;76(1):43-49.

77. Zeydan B, Deelchand DK, Tosakulwong N, et al. Decreased glutamate levels in patients with amnestic mild cognitive impairment: an sLASER proton MR spectroscopy and PiB-PET study. *J Neuroimaging*. 2017;27(6):630-636.

78. Joers JM, Deelchand DK, Lyu T, et al. Neurochemical abnormalities in premanifest and early spinocerebellar ataxias. *Ann Neurol*. 2018;83(4):816-829.

79. Holmay MJ, Terpstra M, Coles LD, et al. N-acetylcysteine boosts brain and blood glutathione in Gaucher and Parkinson diseases. *Clin Neuropharmacol*. 2013;36(4):103-106.

80. Singh N, Sharpley AL, Emir UE, et al. Effect of the putative lithium mimetic ebselen on brain myo-inositol, sleep, and emotional processing in humans. *Neuropsychopharmacology*. 2016;41(7):1768-1778.

81. Wiegers EC, Rooijackers HM, Tack CJ, Heerschap A, de Galan BE, van der Graaf M. Brain lactate concentration falls in response to hypoglycemia in patients with type 1 diabetes and impaired awareness of hypoglycemia. *Diabetes*. 2016;65(6):1601-1605.

82. Seaquist ER, Moheet A, Kumar A, et al. Hypothalamic glucose transport in humans during experimentally induced hypoglycemia-associated autonomic failure. *J Clin Endocrinol Metab*. 2017;102(9):3571-3580.

83. Bednarik P, Tkáč I, Giove F, et al. Neurochemical responses to chromatic and achromatic stimuli in the human visual cortex. *J Cereb Blood Flow Metab*. 2018;38(2):347-359.

84. Kuhn S, Schubert F, Mekle R, et al. Neurotransmitter changes during interference task in anterior cingulate cortex: evidence from fMRI-guided functional MRS at 3 T. *Brain Struct Funct*. 2016;221(5):2541-2551.

85. Bachtiar V, Johnstone A, Berrington A, et al. Modulating regional motor cortical excitability with noninvasive brain stimulation results in neurochemical changes in bilateral motor cortices. *J Neurosci*. 2018;38(33):7327-7336.

SUPPORTING INFORMATION

Additional supporting information may be found online in the Supporting Information section at the end of the article.